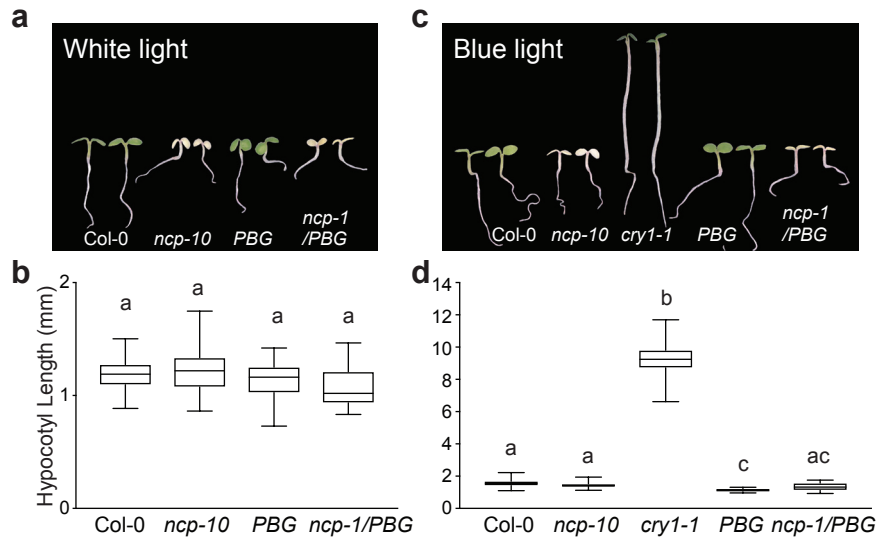
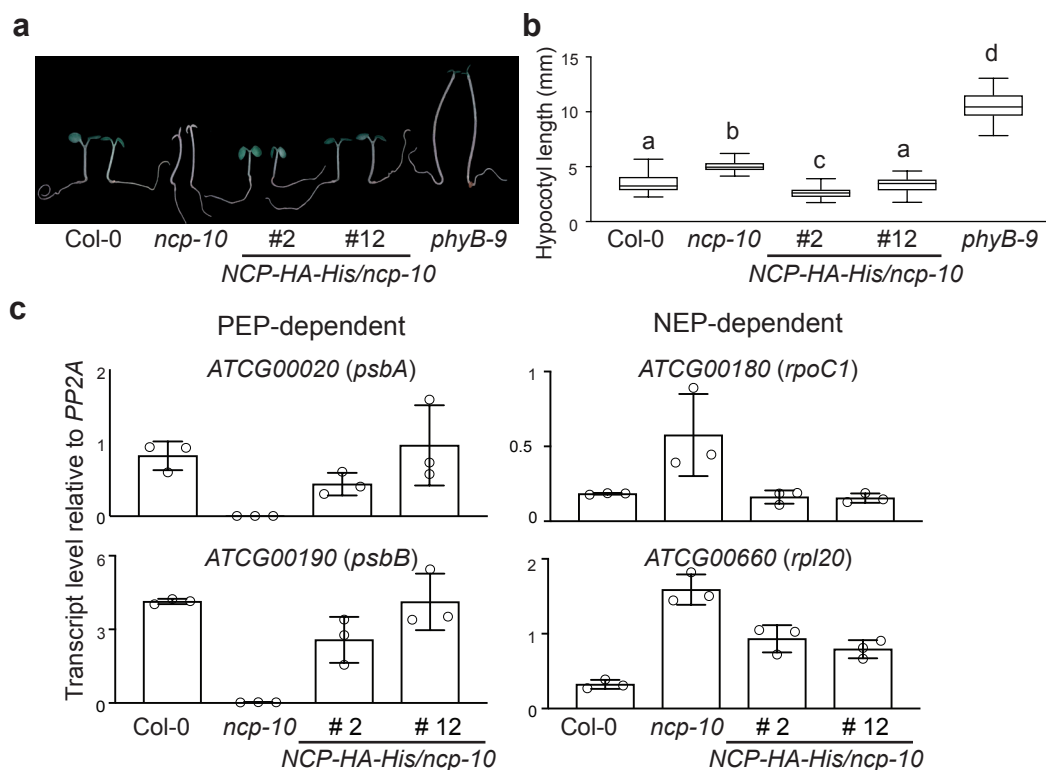


Supplementary Fig. 1. Expressing HA and His tagged *At2g31840*, *NCP-HA-His*, rescues *ncp-1/PBG*. **a**, Representative images of 4-day-old *PBG*, *ncp-1/PBG*, and *NCP-HA-His/ncp-1/PBG* seedlings grown in $10 \mu\text{mol m}^{-2} \text{s}^{-1}$ R light. **b**, Box-and-whisker plot showing hypocotyl length measurements for seedlings from **a**. The boxes represent from the 25th to the 75th percentiles, the bars equal the median values. Samples with different letters have statistically significant differences in hypocotyl length (ANOVA, Tukey's HSD, $p \leq 0.0001$, $n > 20$). **c**, qRT-PCR analyses of the steady-state mRNA levels of *NCP* in 4-d-old *PBG*, *ncp-1/PBG*, *Col-0*, and *ncp-10* seedlings grown under $10 \mu\text{mol m}^{-2} \text{s}^{-1}$ R light. Schematic of the intron-exon structure of *NCP* with the position of mutations are shown. The position for qPCR primers (FP and RP) is located with arrows. The transcript levels of *NCP* were calculated relative to those of *PP2A*. Error bars represent SD of three biological replicates. Asterisks indicate a statistically significant difference in the transcript levels of the bridged columns (Student's *t*-test, **, $p \leq 0.01$, *** $p \leq 0.001$). The source data underlying the hypocotyl measurements in **b** and the qRT-PCR data in **c** are provided in the Source Data file.



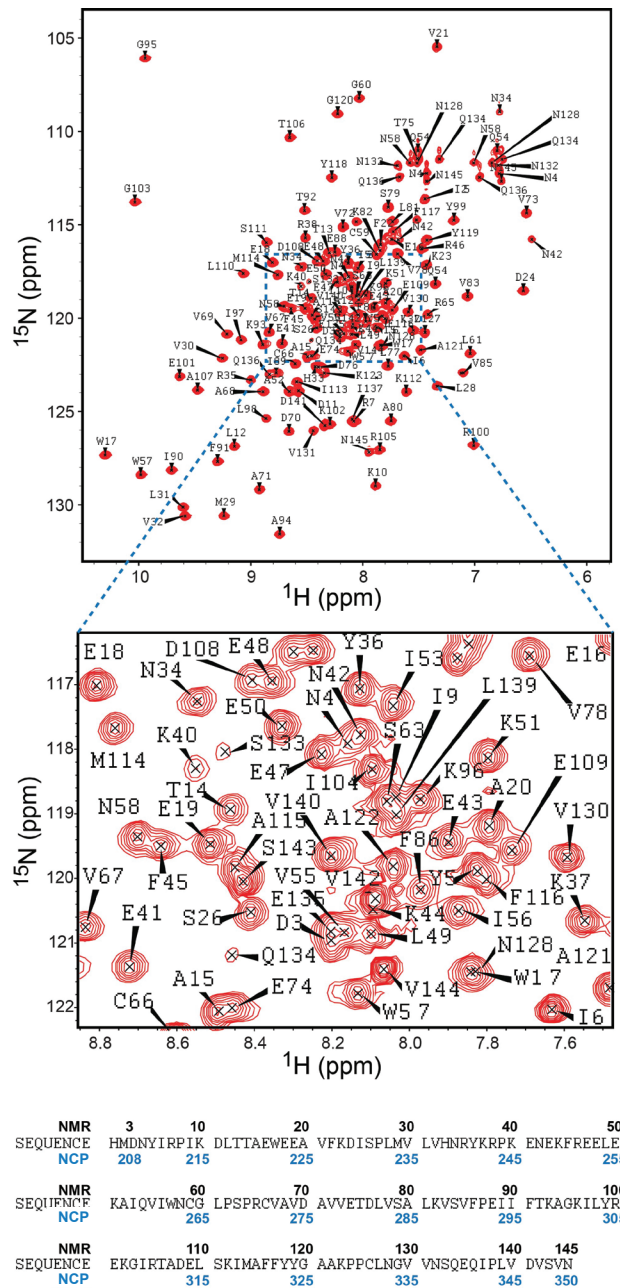
Supplementary Fig. 2. *ncp* mutants exhibit normal hypocotyl responses to blue and white light.

a, Representative images of 4-d-old Col-0, *ncp-10*, PBG, and *ncp-1/PBG* seedlings grown in $33 \mu\text{mol m}^{-2} \text{s}^{-1}$ white light. **b**, Box-and-whisker plots for hypocotyl length measurements of seedlings in **a**. **c**, Representative images of 4-d-old Col-0, *ncp-10*, *cry1-1*, PBG, and *ncp-1/PBG* seedlings grown in $10 \mu\text{mol m}^{-2} \text{s}^{-1}$ blue light. **d**, Box-and-whisker plots for hypocotyl length measurements of seedlings in **c**. For **b** and **d**, the boxes represent from the 25th to the 75th percentiles, and the bars equal the median values. Samples with different letters indicate statistically significant differences in hypocotyl length (ANOVA, Tukey's HSD, $p \leq 0.001$, $n > 40$). The source data underlying the hypocotyl measurements in **b** and **d** are provided in the Source Data file.



Supplementary Fig. 3. Expressing HA and His tagged *NCP-HA-His* rescues *ncp-10*.

a, Representative images of 4-d-old Col-0, *ncp-10*, *NCP-HA-His/ncp-10* line #2 and #12, and *phyB-9* seedlings grown in $10 \mu\text{mol m}^{-2} \text{s}^{-1}$ R light. **b**, Box-and-whisker plots showing hypocotyl length measurements of seedlings from **a**. The boxes represent from the 25th to the 75th percentiles, and the bars equal the median values. Samples with different letters exhibit statistically significant difference in hypocotyl length (ANOVA, Tukey's HSD, $p \leq 0.001$, $n > 30$). **c**, qRT-PCR analyses of the steady-state mRNA levels of selected PEP-dependent and NEP-dependent genes in 4-d-old Col-0, *ncp-10*, *ncp-10/NCP-HA-His* #2, and *ncp-10/NCP-HA-His* #12 grown in $10 \mu\text{mol m}^{-2} \text{s}^{-1}$ R light. Transcript levels were calculated relative to those of *PP2A*. Error bars represent SD of three biological replicates. The source data underlying the hypocotyl measurements in **b** and the qRT-PCR data in **c** are provided in the Source Data file.

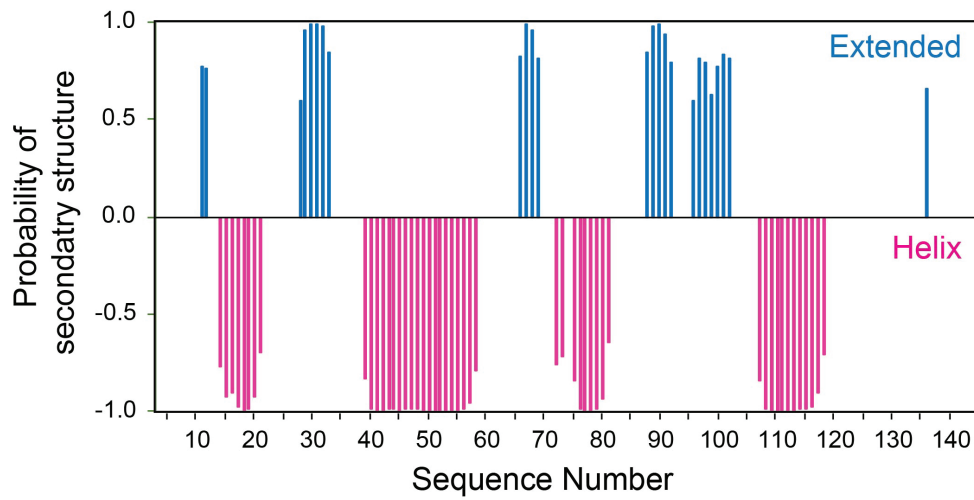


Supplementary Fig. 4. ^1H - ^{15}N HSQC spectrum of the NCP Trx-like domain.

The sequence of the NMR construct is shown below the NMR spectrum. Resonance assignments of individual signals reflect the residue numbers within the NMR construct. The residue numbers within the full-length NCP protein are labeled in blue beneath the sequence.

a

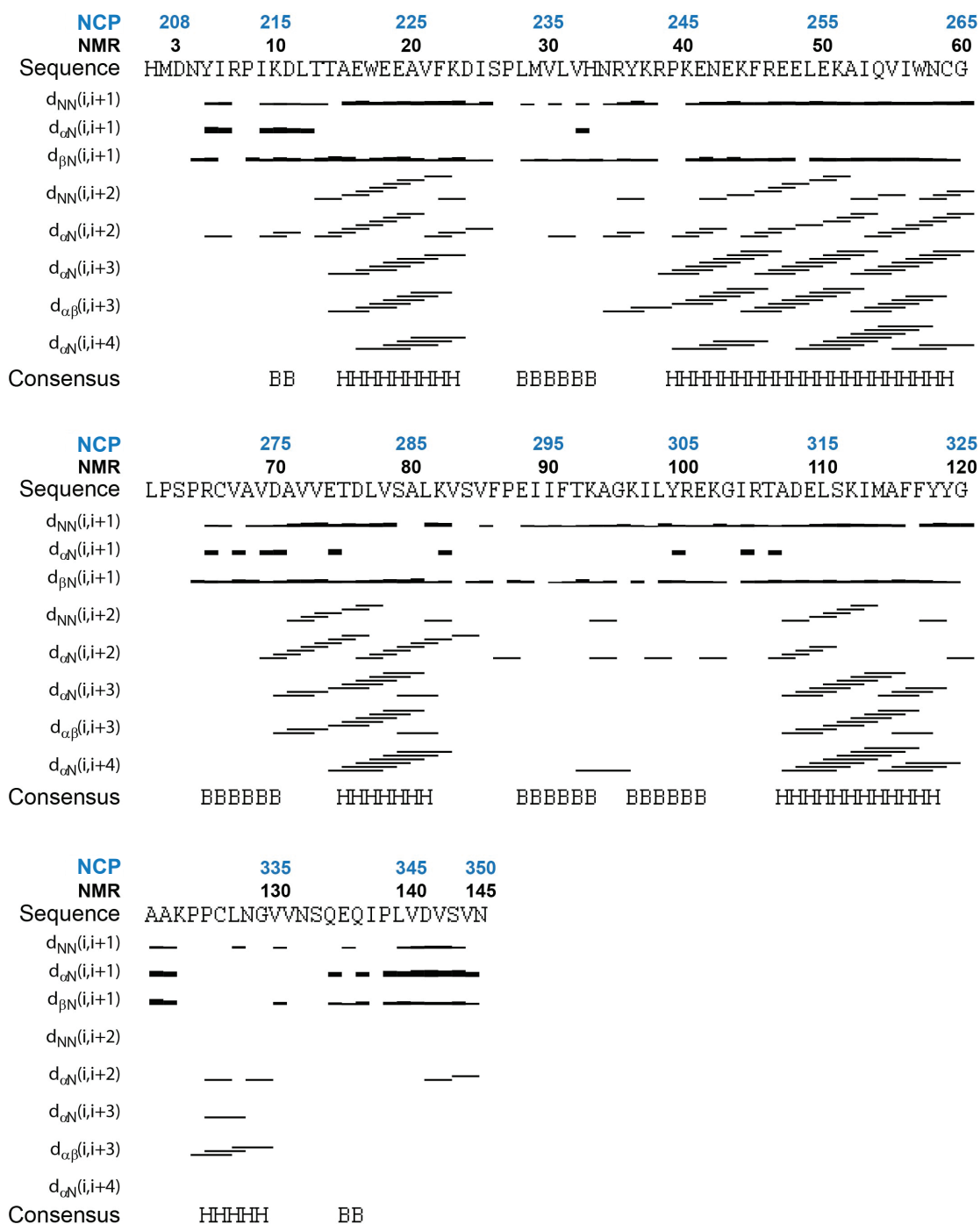
Neural network secondary structure prediction
based on chemical shift indices (CSI)

**b**

NCP		208	215	225	235	245	255
NMR		3	10	20	30	40	50
SEQUENCE		DNYIRPIK	DLTTAEWEEA	VFKDISPLMV	LVHNRYKRPK	ENEKFREELE	
PREDICTED_SS		LLLLLLL	EELHHHHH	HLLLLLEE	EELLLLLH	HHHHHHH	
CONFIDENCE		08899984	5545889998	3478997199	9966899869	9999999999	
NCP		265	275	285	295	305	
NMR		60	70	80	90	100	
SEQUENCE		KAIQVIWNCG	LPSPRCVAVD	AVVETDLVSA	LKVSVFPEII	FTKAGKILYR	
PREDICTED_SS		HHHHHHHLL	LLLLLEEL	LHHLHHHHH	HLLLLLEE	EELLEEEEE	
CONFIDENCE		9999999548	9998669965	6543699998	2689551699	8507716525	
NCP		315	325	335	345	350	
NMR		110	120	130	140	145	
SEQUENCE		EKGIRTADEL	SKIMAFFYYG	AAKPPCLNGV	VNSQEIQPLV	DVSVN	
PREDICTED_SS		EELLLLHHH	HHHHHHHLL	LLLLLLLLL	LLLLLELLL	LLLLL	
CONFIDENCE		6636687999	9999997468	9999879971	6898236778	88880	

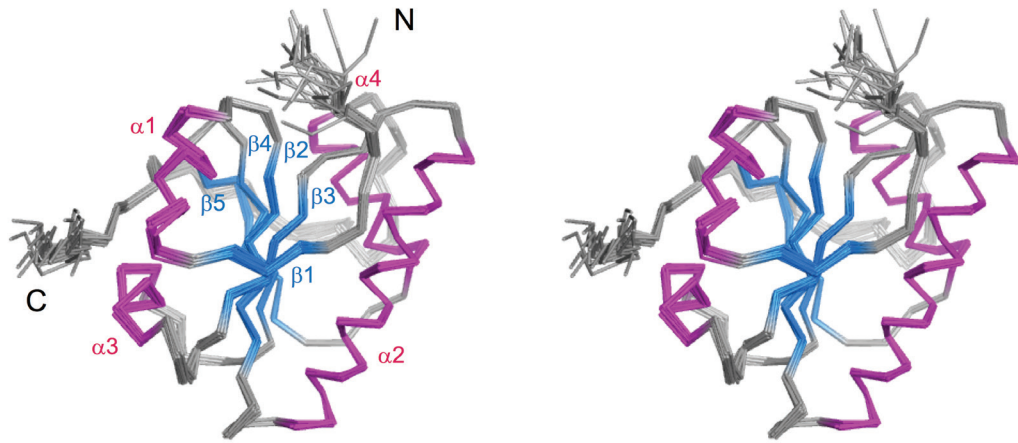
Supplementary Fig. 5. Secondary structure analysis of the NCP Trx-like domain.

a, Neural network secondary structure prediction based on the chemical shift indices (CSI) analysis of the NCP Trx-like domain. The probability of each residue adopting an extended or helical conformation is plotted in blue or pink, respectively. **b**, The predicted secondary structures and confidence levels along the primary protein sequence. Residue numbers in the NMR construct and full-length NCP are colored in black and blue respectively. Residues predicted in the extended conformation are colored in blue, while those in the helical conformation are colored in pink.



Supplementary Fig. 6. Secondary structure determination of the NCP Trx-like domain based on the NOE pattern.

The presence of β -strands (extended conformations) is reflected by very strong NOE signals of $d_{\alpha N}(i, i+1)$ (indicated by thick bars), whereas the presence of helices is reflected by the characteristic NOEs of $d_{\alpha\beta}(i, i+3)$, $d_{\alpha N}(i, i+3)$ and $d_{\alpha N}(i, i+4)$.



Supplementary Fig. 7. A stereo view of the NMR structural ensemble of the NCP Trx-like structures. Alpha-helices and beta-strands are colored in magenta and blue, respectively.

Supplementary Table 1. Primers used for making plasmid constructs

Accession	Gene name	Vector name	Forward primer	Reverse primer
<i>At2g31840</i>	<i>NCP-HA-His</i>	pCHF1	TTCTTCTATAAAAACAATACCATGATTCTTCCATTTTCGACACAGTTC ACTTGC	GGGGGTGGGGGTGGGGGTGGGGGTGGGATTCACACTTACA TCGACTAAAGG
<i>At2g31840</i>	<i>NCP-CGP-Flag</i>	pCHF3	ACGGGGGACGAGCTCGGTACCCGGGATGATTCTTCCATTTTCGAC	GTGTTGGAGTAGGCTCTAGAATATTCACACTTACATCGACTA
<i>At2g31840</i>	<i>NCP-FL</i>	pCMX-PL2	TCGAGAAGCTTGATATCGAATTCATGATTCTTCCATTTTCGAC	TACTAGCTAGCTGGCCAGGATCCTCAGTGATGGTGATGGTG
<i>At2g31840</i>	<i>NCPΔ48</i>	pCMX-PL2	TCGAGAAGCTTGATATCGAATTCATGTCCTCCTCGAAGTGG	TACTAGCTAGCTGGCCAGGATCCTCAGTGATGGTGATGGTG
<i>At2g31840</i>	<i>NCP-FL</i>	pET15b	ATACATATGATGATTCTTCCATTTTC	TTGCTCGAGTTAATTCACACTTACATCGAC
<i>At2g31840</i>	<i>NCPΔ206</i>	pET15b	TAACATATGGGAGATGATAGTGAGAAGGA	TTGCTCGAGTTAATTCACACTTACATCGAC
<i>At4g28590</i>	<i>RCBΔ98</i>	pET28a	CAGCAAATGGGTCGCGCTAGTGAAGCAGACGCTGTG	CTCGAGTGC GGCCGCACTAACAGTACGGGGTTAC
<i>At4g28590</i>	<i>RCBΔ197</i>	pET28a	CAGCAAATGGGTCGCGCTGAGATTGATGATAGTTGGG	CTCGAGTGC GGCCGCACTAACAGTACGGGGTTAC

Supplementary Table 2. qRT-PCR primers for the plastidial-encoded genes examined in this study

Accession	Gene name	Primer for cDNA synthesis	Primer pair for qRT-PCR
ATCG00020	<i>psbA</i>	TAGATGGAGCCTCAACAGCAGCTA	ACATTTCTTCTTAGCGGCTT CGTCCTTGACTATCAACTACTGA
ATCG00680	<i>psbB</i>	CATCCAAATCTGGATCAATACCAG	ACATTTCTTCTTAGCGGCTT CGTCCTTGACTATCAACTACTGA
ATCG00490	<i>rbcL</i>	CTTCACAAGCAGCAGCTAGTTCAGG	GGAGATGATTCTGTACTACAAT GTCCCTCATTACGAGCTTGTAC
ATCG00190	<i>rpoB</i>	CAATGATAGTGGTACCAAGTACTTC	CTAGTGGACATTATGCACTTGT CAGATTTATAAGTAAGCATCTCTTG
ATCG00180	<i>rpoC1</i>	GTATAGCTTCCTCGATTTCTCG	GATGCAATTGGAGCTTATCG CGATAGGAACTTCTCTTGAAGC
ATCG00660	<i>rpl20</i>	TGTGCAAGTATTTTCCGATTAAG	GAGCTTTAGTTTCGGCTCATC AATTACGGCATTATTTCGAGTG

Supplementary Table 3. qRT-PCR primers for the nuclear genes examined in this study.

Accession	Gene name	Forward primer	Reverse primer
AT1G69960	<i>PP2A</i>	TATCGGATGACGATTCTTCGTGCAG	GCTTGGTCGACTATCGAATGAGAG
AT2G31840	<i>NCP</i>	GAAGCGAGTCTCGATGATCC	GCTTCTGCATCTTCCTCCTC

Supplementary Table 4. Gene ID or transcript ID for phylogenetic analysis of NCP and RCB homologues.

Taxas	Gene name	Gene ID	Transcript Identifier	PAC ID	Source	1KP Identifier
Angiosperm						
<i>Amborella trichopoda</i>	NCP	ATR_00066G00940	evm_27.model.AmTr_v1.0_sc affold00066.94 CDS	-	Genome, Amborella Genome Project	-
	RCB	ATR_00066G01920	evm_27.model.AmTr_v1.0_sc affold00066.192 CDS	-		Genome, Amborella Genome Project
<i>Arabidopsis thaliana</i>	NCP	AT2G31840.1	-	19643553	Genome, Phytozome	-
	RCB	AT4G28590.1	-	19645001		Genome, Phytozome
<i>Oriza sativa</i>	NCP	LOC_Os05g34470	-	24152372	Genome, Phytozome	-
	RCB	LOC_Os01g61320	-	24114913		Genome, Phytozome
Gymnosperm						
<i>Ginkgo biloba</i>	NCP	-	SGTW_scaffold_2001407 Ginkgo_biloba	-	Transcriptome, 1KP	SGTW
	RCB	-	SGTW_scaffold_2037234 Ginkgo_biloba	-		Transcriptome, 1KP
<i>Picea abies</i>	NCP	MA_875929	-	-	Congenie, Genome	-
	RCB	MA_85974	-	-		Congenie, Genome
<i>Gnetum montanum</i>	NCP	GMO00014786	GTHK-0020791-2011195- Gnetum_montanum_987	-	Transcriptome, 1KP	GTHK
	RCB	GMO00015329	GTHK-2055953-0021387- Gnetum_montanum_1122	-		Transcriptome, 1KP
Fern						
<i>Equisetum diffusum</i>	NCP/RCB	-	CAPN-1001418-2006808- Equisetum_diffusum_996	-	Transcriptome, 1KP	CAPN

<i>Psilotum nudum</i>	NCP/RCB	-	QVMR-2010863-0072637- Psilotum_nudum_1272	-	Transcriptome, 1KP	QVMR
<i>Angiopteris evecta</i>	NCP/RCB	-	NHCM-0020880-2008213- Angiopteris_evecta	-	Transcriptome, 1KP	NHCM
Lycophytes						
<i>Selaginella moellendorffii</i>	NCP/RCB	SM00002G04620	404435	-	Genome, Phytozome	-
<i>Pseudolycopodiella caroliniana</i>	NCP/RCB	-	UPMJ-2011768-0026604- Pseudolycopodiella_caroliniana_1203	-	Transcriptome, 1KP	UPMJ
Hornwort						
<i>Nothoceros vincentianus</i>	NCP/RCB	-	TCBC-2019434-0029159- Nothoceros_vincentianus_1187	-	Transcriptome, 1KP	TCBC
Liverwort						
<i>Sphaerocarpos texanus</i>	NCP/RCB	-	HERT-0056768-2043911- Sphaerocarpos_texanus_930	-	Transcriptome, 1KP	HERT
Moss						
<i>Physcomitrella patens</i>	NCP/RCB	Pp3c3_26500	PHYPADRAFT_172419	-	Genome, Phytozome	-

"-" indicates not applicable.